

DEVELOPMENT OF CONTACTLESS RESONANT MEMS FORCE SENSORS IN SOI TECHNOLOGY

B. Andò¹, S. Baglio¹, N. Savalli¹, C. Trigona¹

¹ DIEES, University of Catania, Catania, Italy.

*Corresponding author: Salvatore Baglio, tel.: +39-095-7382325, fax: +39-095-330793
salvatore.baglio@diees.unict.it

M. Baù², V. Ferrari², D. Marioli², E. Sardini², M. Serpelloni²

²Department of Electronics for Automation, University of Brescia, Brescia, Italy.

Abstract: In this paper an innovative micromachined resonant force sensor, based on magnetic remote readout and actuation strategy is presented. The device resonance frequency changes in presence of the compressive axial-force to be measured due to changes in the device elastic properties; the sensor is driven to resonance by using externally induced Lorentz forces and the output is then obtained via an inductive pick-up.

Keywords: resonant force sensor, contactless sensor, MEMS.

THE SOI FORCE SENSOR

Load cells and force sensors are generally based on bonded-foil strain gauges or piezo-resistive materials whose resistance changes when an external force is applied. These devices cannot be used in harsh environments and represent an incompatible solution for contactless and not-wired measurement systems. The microsensor presented in this work represents an innovative passive force sensor that can be interrogated adopting a remote sensing strategy: the actuation principle of the architecture proposed is based on the interaction between the eddy currents and the magnetic field generated by an external inductor driven by a sinusoidal signal; the system response (correlated to compressive axial-force) is analyzed adopting a remotely sensing system based on an inductive sensor [1].

THE STRESS SENSOR MODEL

In the following the procedure to obtain the resonant frequency changes, as a function of the applied axial load force (S), is briefly described using the elastic beam theory (Figure 1).

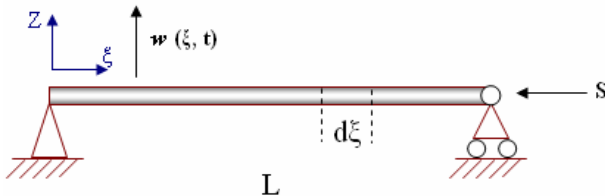


Figure 1. Beam under axial load force.

According to Figure 2 the balance equation along the z-axis, if the higher order terms are neglected, is given by eq. (1):

$$-T - md\xi \frac{\partial^2 w}{\partial t^2} + T + dT - S \sin \varphi_1 + S \sin \varphi_2 = 0 \quad (1)$$

where the φ_1 , φ_2 are the angles at the initial position ξ and $\xi+d\xi$, respectively, T is the shear force and M is the moment.

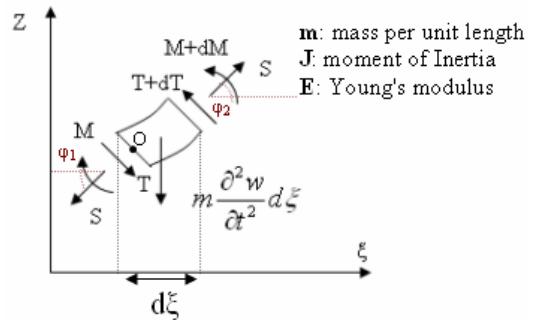


Figure 2. Force analysis.

The linearization at a static equilibrium point allows to define the left and right displacements, respectively:

$$w_L(\xi, t) = w(\xi, t)$$

$$w_R(\xi, t) = w(\xi, t) + dw(\xi, t) = w(\xi, t) + \left(\frac{\partial w(\xi, t)}{\partial \xi} \right) d\xi \quad (2)$$

where dw represents the incremental displacement as shown in Figure 3.

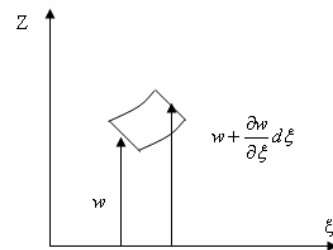


Figure 3. Incremental displacement analysis.

For small displacement (φ_1 and φ_2 are very small), it is possible to write:

$$\sin \varphi_1 \approx \varphi_1 \approx tg \varphi_1 = \frac{\partial w}{\partial \xi} \quad (3)$$

$$\sin \varphi_2 \approx \varphi_2 \approx tg \varphi_2 = \frac{\partial}{\partial \xi} \left(w + \frac{\partial w}{\partial \xi} d\xi \right) = \frac{\partial w}{\partial \xi} + \frac{\partial^2 w}{\partial \xi^2} d\xi$$

that replaced in the expression (1) gives:

$$\frac{\partial T}{\partial \xi} d\xi - m \frac{\partial^2 w}{\partial t^2} d\xi + S \frac{\partial^2 w}{\partial \xi^2} d\xi = 0 \quad (4)$$

The dynamic rotation around the point O can be written as follows:

$$T(\xi, t) = - \left(\frac{\partial M(\xi, t)}{\partial \xi} \right) \Rightarrow \frac{\partial T(\xi, t)}{\partial \xi} = - \frac{\partial^2 M(\xi, t)}{\partial \xi^2} \quad (5)$$

Replacing the expression (5) in the expression (4), the following equation can be obtained:

$$- \left(\frac{\partial^2 M(\xi, t)}{\partial \xi^2} \right) d\xi - m \frac{\partial^2 w(\xi, t)}{\partial t^2} d\xi + S \frac{\partial^2 w(\xi, t)}{\partial \xi^2} d\xi = 0 \quad (6)$$

Taking into consideration the Eulero-Bernoulli beam theory and under the hypothesis of homogeneous beam ($EJ = \text{constant}$), a fourth-order differential equation can be obtained to describe the motion beam (w) subjected to a static axial load S :

$$- EJ \left(\frac{\partial^4 w}{\partial \xi^4} \right) + S \left(\frac{\partial^2 w}{\partial \xi^2} \right) = m \frac{\partial^2 w}{\partial t^2} \quad (7)$$

Assuming a particular integral of the form:

$$w(\xi, t) = \psi_c(\xi) G(t) \quad (8)$$

that replaced in expression (7) gives the following differential equation:

$$EJ \frac{d^4 \psi_c(\xi)}{d\xi^4} G(t) - S \frac{d^2 \psi_c(\xi)}{d\xi^2} G(t) + m \psi_c(\xi) \frac{d^2 G(t)}{dt^2} = 0 \quad (9)$$

Then, it is possible to define two different ordinary differential equations, to obtain $G(t)$ and $\psi_c(\xi)$, respectively:

$$w(\xi, t) = \psi_c(\xi) G(t) = (F_1 \sin \gamma_1 \xi + F_2 \cos \gamma_1 \xi + F_3 \sinh \gamma_2 \xi + F_4 \cosh \gamma_2 \xi) (A \sin \omega t + B \cos \omega t) \quad (10)$$

with:

$$\gamma_1 = \sqrt{-\frac{S - \sqrt{S^2 + 4EJm\omega^2}}{2EJ}}$$

$$\gamma_2 = \sqrt{\frac{S + \sqrt{S^2 + 4EJm\omega^2}}{2EJ}} \quad (11)$$

whereas F_1, F_2, F_3, F_4 are strictly related to the boundary conditions and A, B correlated to the initial condition of the system at $t=0$; thus, taking into account the Figure 1, they can be expressed as:

$$\begin{aligned} [w(\xi, t)]_{\xi=0} &= 0 \\ [w(\xi, t)]_{\xi=L} &= 0 \\ [M]_{\xi=0} &= EJ \left[\frac{\partial^2 w}{\partial \xi^2} \right]_{\xi=0} = 0 \Rightarrow F_2, F_3, F_4 = 0; \quad F_1 = 1 \\ [M]_{\xi=L} &= EJ \left[\frac{\partial^2 w}{\partial \xi^2} \right]_{\xi=L} = 0 \end{aligned}$$

$$\begin{aligned} \Rightarrow w(\xi, t) &= (\sin \gamma_1 \xi) (A \sin \omega t + B \cos \omega t) = \\ &= \left(\sin \frac{\pi}{L} \xi \right) (A \sin \omega t + B \cos \omega t) \end{aligned} \quad (12)$$

Equation (12) represents the beam motion model subjected to an axial load S . The frequency response as function of the applied axial load, which is represented in Figure 4, can be expressed adopting equations (11) [2]:

$$\gamma_1^2 = \frac{\pi^2}{L^2} = -\frac{S - \sqrt{S^2 + 4EJm\omega^2}}{2EJ} \quad (13)$$

$$\Rightarrow f_r \cong \frac{1}{2L} \sqrt{\frac{\left(S + EJ \left(\frac{\pi^2}{L^2} \right) \right)}{m}} \quad (14)$$

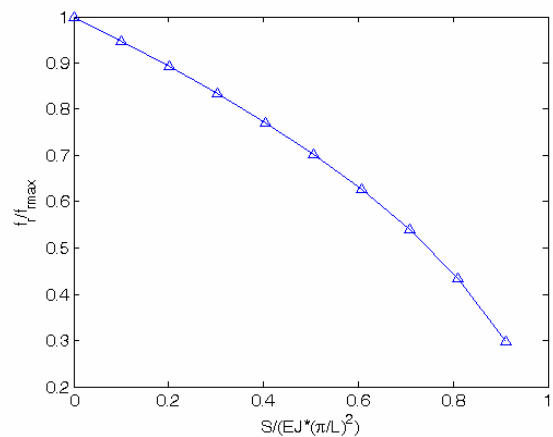


Figure 4. Frequency response as a function of the applied axial load (S).

THE SOI DESIGN PROTOTYPE

The force sensor has been developed by adopting a BESOI (Bulk and Etch Silicon on Insulator) technology, thus releasing a symmetric device (with aluminium surface) supported by four beams (Figure 5(a)). In order to simulate the physical behaviour of the micromachined device, CoventorWare[®] MemMech tool, based on a FEM method has been used (Figure 5(b) and 5(c)).

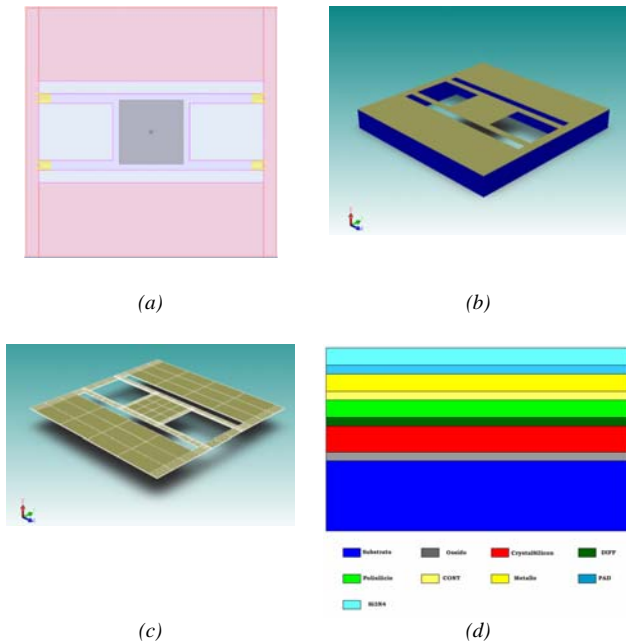


Figure 5. a) Force sensor layout in SOI technology, b) 3D model device, c) CoventorWare[®] mesh model, d) Silicon on Insulator stack materials.

A custom MEMS process has been adopted: SOI-based bulk micromachining (Figure 5(d)). This technology is based on a 450 μm thick carrier silicon substrate, separated from a 15 μm thick c-Si layer by a 2 μm thick buried oxide.

The etching operations of Silicon from both the front side and the bottom side can be summarized as follow:

- a RIE etching on the front-side is used to remove 15 μm of Silicon;
- a DRIE etching of Silicon on the back-side is adopted, in order to remove the 450 μm of silicon;
- a RIE etching of buried SiO_2 from the backside is used to remove the 2 μm of oxide.

Table 1 summarizes the process characteristics.

Substrate (silicon)	450 μm
Oxide	2 μm
Silicon	15 μm
Oxide	0.1 μm
Polysilicon	0.48 μm
Oxide	0.73 μm
Metal	1 μm
Oxide	0.5 μm
Nitride	2 μm

Table 1. Feature of the custom SOI foundry process.

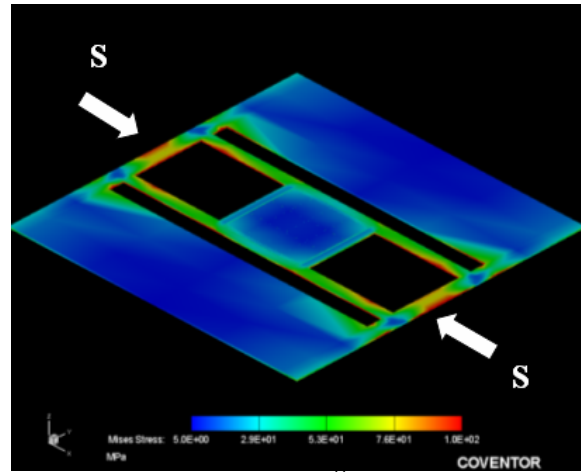


Figure 6. CoventorWare[®] - FEM analysis. The colour map shows the stress distribution.

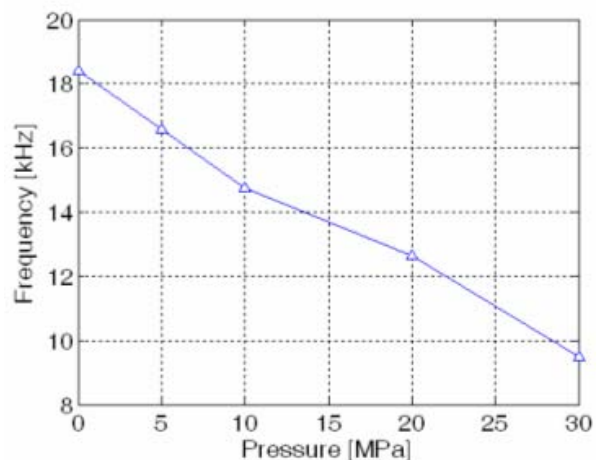


Figure 7. CoventorWare[®] FEM-analysis: resonant frequency as function of the axial load pressure.

THE CONTACTLESS STRATEGY

The contactless working principle is based on Lorentz force actuation system, and a differential dual-coil inductor to measure the device resonance oscillations [3, 4]. Moreover, the interaction between the eddy currents and the magnetic field, generated by an external inductor onto the conductive mass (exerted by a sinusoidal signal) are exploited for the actuation. Furthermore, the system response (strongly depending on the applied external force) is analyzed adopting a remotely sensing based on an inductive sensor. The actuation/sensing process can be summarized as follows:

- 1) a sinusoidal bias signal, having a frequency of $f_r/2$ (f_r : resonance frequency of the mechanical structure), is used to excite the elastic structure;
- 2) a sinusoidal signal at 80 kHz is used to bias the primary coil of the sensing inductor;
- 3) the conditioning circuit output represents the displacement information (AM signal, modulated by the device motion);
- 4) the device frequency response (related to the axial force) can be analyzed using an amplitude demodulator.

In Figure 8 the contactless readout strategy is sketched:

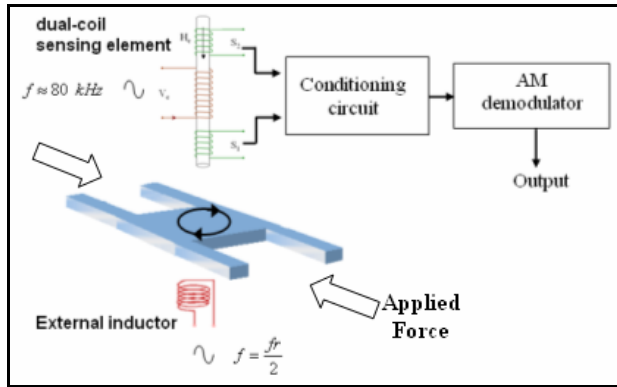
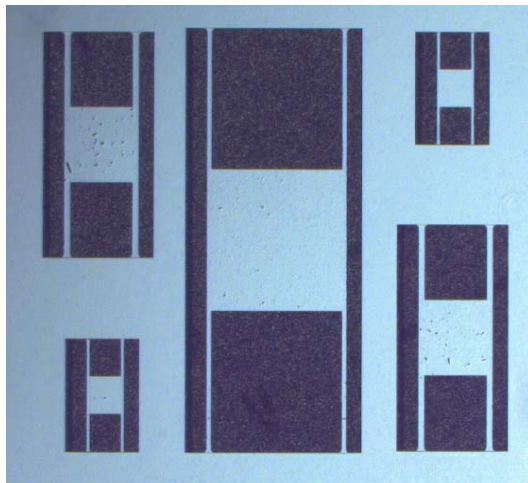
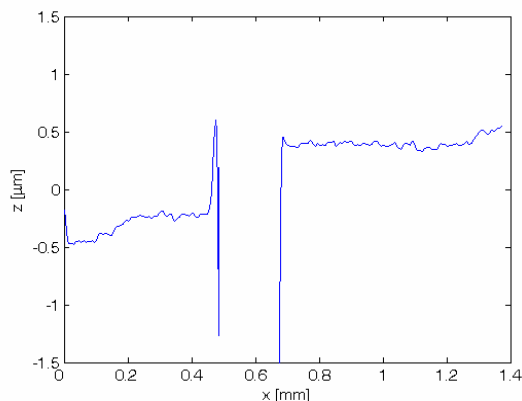


Figure 8. Contactless electromagnetic readout strategy.

The Figure 9(a) shows a microscope picture of a set of SOI force sensors while Figure 9(b) the output of a profile experimental analysis (performed through a confocal microscope).



(a)



(b)

Figure 9. a) SOI force sensor prototypes, b) profile analysis of the central pictured device.

CONCLUSIONS

The development of a novel force sensor for contactless measurements has been described in this work.

A cantilever beam subjected to an axial load has been modeled and the frequency response, as a function of the applied axial load, has been obtained.

The developed force sensor (mainly composed by a central square area supported by four beams) has been simulated using the CoventorWare[®] MemMech solver, based on a FEM method.

The SOI prototypes have been realized adopting a custom MEMS process.

Future activities will include the contactless characterization of the devices, performed by using a Lorentz force actuation principle, and a sensing inductor to measure the system resonance frequency variation as consequence of the external applied axial load.

REFERENCES

1. M. Baù, V. Ferrari, D. Marioli, E. Sardini, M. Serpelloni, A. Taroni; *Contactless Excitation and Readout of Passive Sensing Elements Made by Miniaturized Mechanical Resonators*, IEEE Sensors 2007, 28-31 Oct. 2007, pp 36-39.
2. C. Cho, Y. Park, *Frequency tuning of the MEMS device: the changing the natural frequency by imposing the axial force*, 6th Korea-Japan Symposium of Frontiers in Vibration Science and Technology, Ibaraki University, July 14-15, 2005.
3. C. De Angelis, V. Ferrari, D. Marioli, E. Sardini, M. Serpelloni, A. Taroni ; *Magnetically induced oscillations on a conductive cantilever for resonant microsensors*, Sensors and Actuators A 135, 2007, pp 197-202.
4. M. Baù, M. Motterlini, V. Ferrari, D. Marioli, A. Taroni, *Contactless system for dynamic characterization of microresonator*, Electronics letters, 27th April 2006, Vol. 42 No. 9.